

This paper was presented at the colloquium “Computational Biomolecular Science,” organized by Russell Doolittle, J. Andrew McCammon, and Peter G. Wolynes, held September 11–13, 1997, sponsored by the National Academy of Sciences at the Arnold and Mabel Beckman Center in Irvine, CA.

Architecture and mechanism of the light-harvesting apparatus of purple bacteria

XICHE HU, ANA DAMJANOVIĆ, THORSTEN RITZ, AND KLAUS SCHULTEN

Beckman Institute and Department of Physics, University of Illinois at Urbana–Champaign, Urbana, IL 61801

ABSTRACT Photosynthetic organisms fuel their metabolism with light energy and have developed for this purpose an efficient apparatus for harvesting sunlight. The atomic structure of the apparatus, as it evolved in purple bacteria, has been constructed through a combination of x-ray crystallography, electron microscopy, and modeling. The detailed structure and overall architecture reveals a hierarchical aggregate of pigments that utilizes, as shown through femtosecond spectroscopy and quantum physics, elegant and efficient mechanisms for primary light absorption and transfer of electronic excitation toward the photosynthetic reaction center.

The prevalent color green in Earth’s biosphere is testimony to the important role that chlorophylls play in harnessing the energy of the Sun to fuel the metabolism of photosynthetic life forms. Chlorophylls are assisted in their light-harvesting role by carotenoids, also widely known through their coloration of petals and fruits in plants. Photosynthetic organisms have evolved intricate aggregates of chlorophylls and carotenoids for efficient light harvesting and exploit in subtle ways the laws of quantum mechanics. This role of chlorophylls and carotenoids has emerged in full detail only recently, when the atomic structures of proteins involved in bacterial photosynthetic light harvesting have been solved by a combination of x-ray crystallography, electron microscopy, and molecular modeling.

However, the conceptual foundation for our present understanding of light harvesting was laid long ago, when Emerson and Arnold demonstrated that it required hundreds of chlorophylls to reduce one molecule of CO₂ under saturating flash light intensity (1, 2). To explain the cooperative action of these chlorophylls, Emerson and Arnold postulated that only very few chlorophylls in the primary reaction site, termed the photosynthetic reaction center (RC), directly take part in photochemical reactions; most chlorophylls serve as light-harvesting antennae by capturing the sunlight and funneling electronic excitation toward the RC. This notion gave rise to the definition of the photosynthetic unit (PSU) as an ensemble of an RC with associated light-harvesting complexes containing up to 250 chlorophylls, and became widely accepted only when Duysens carried out a critical experiment in which energy transfer between different chlorophylls was observed (3).

A wealth of accumulated evidence proves that the organization of PSUs, to surround an RC with aggregates of chlorophylls and associated carotenoids, is universal in both photosynthetic bacteria and higher plants (2, 4–6).

Of the known photosynthetic systems, the PSU of purple bacteria is the most studied and best characterized. Fig. 1 depicts schematically the intracytoplasmic membrane of purple bacteria with its primary photosynthetic apparatus. In the

PSU, an array of light-harvesting complexes captures light and transfers the excitation energy to the photosynthetic RC. This article focuses on the primary processes of light harvesting and electronic excitation transfer that occur in the PSU, and describes the role of molecular modeling in elucidating the underlying mechanisms.

In most purple bacteria, the photosynthetic membranes contain two types of light-harvesting complexes, light-harvesting complex I (LH-I) and light-harvesting complex II (LH-II) (7). LH-I is found surrounding directly the RCs (8, 9), whereas LH-II is not in direct contact with the RC but transfers energy to the RC through LH-I (10, 11). For some bacteria, such as *Rhodospseudomonas (Rps.) acidophila* and *Rhodospirillum (Rs.) molischianum* strain DSM 120 (12), there exists a third type of light-harvesting complex, LH-III. A 1:1 stoichiometry exists between the RC and LH-I (9); the number of LH-IIs and LH-IIIs varies according to growth conditions such as light intensity and temperature (13).

Purple bacteria absorb light in a spectral region complementary to that of plants and algae, mainly at wavelengths of about 500 nm through carotenoids and above 800 nm through bacteriochlorophylls (BChls). Fig. 2 shows the energy levels for the key electronic excitations in the PSU. There exists a pronounced energetic hierarchy in the light-harvesting system: LH-III absorbs light at the highest energy (800 and 820 nm); the LH-II complex, which surrounds LH-I, absorbs maximally at 800 nm and 850 nm; and LH-I, which in turn surrounds the RC, absorbs at a lower energy (875 nm) (11). The energy cascade serves to funnel electronic excitations from the LH-IIIs and LH-IIIs through LH-I to the RC. Time resolved picosecond and femtosecond spectroscopy revealed that excitation transfer within the PSU occurs on a subpicosecond time scale and at near unit (95%) efficiency (14, 15).

Today, structures of the major components of the bacterial photosynthetic apparatus are available at atomic resolution. Structures of the RC are known for *Rps. viridis* (16) as well as for *Rhodobacter (Rb.) sphaeroides* (17). Recently, high resolution crystal structures of LH-II have been determined for *Rps. acidophila* (18) and for *Rs. molischianum* (19). Based on a high degree of homology of the $\alpha\beta$ -heterodimer of LH-I from *Rb. sphaeroides* to that of LH-II of *Rs. molischianum* (12, 20), an atomic structure for LH-I of *Rb. sphaeroides* has been modeled (21).

Structure of Light-Harvesting Complexes

Accordingly, a structural model for the bacterial PSU has been established and consists of LH-IIs, LH-I, and the RC; this model provides detailed knowledge of the organization of

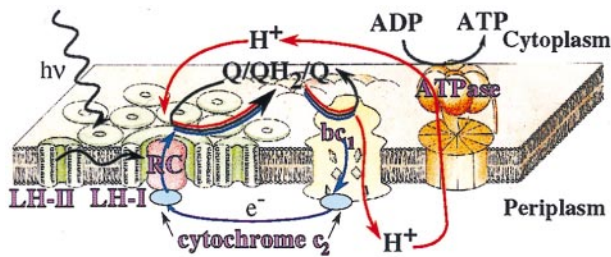


FIG. 1. Schematic representation of the photosynthetic apparatus in the intracytoplasmic membrane of purple bacteria. The RC (red) is surrounded by the light-harvesting complex I (LH-I, green) to form the LH-I-RC complex, which is surrounded by multiple light-harvesting complexes LH-II (green), forming altogether the PSU. Photons are absorbed by the light-harvesting complexes and excitation is transferred to the RC initiating a charge (electron-hole) separation. The RC binds quinone Q_B , reduces it to hydroquinone Q_BH_2 , and releases the latter. Q_BH_2 is oxidized by the bc_1 complex, which uses the exothermic reaction to pump protons across the membrane; electrons are shuttled back to the RC by the cytochrome c_2 complex (blue) from the ubiquinone-cytochrome bc_1 complex (yellow). The electron transfer across the membrane produces a large proton gradient that drives the synthesis of ATP from ADP by the ATPase (orange). Electron flow is represented in blue, proton flow in red, and quinone flow, likely confined to the intramembrane space, in black.

chromophores in the photosynthetic membrane and opens a door to the study of excitation transfer in the PSU based on *a priori* principles.

LH-II. The structure of LH-II from *Rs. molischianum* had been determined to 2.4 Å resolution (19) and is shown in Fig. 3*a*. The complex is an octameric aggregate of $\alpha\beta$ -heterodimers; the latter contains a pair of short peptides (α - and β -apoproteins) noncovalently binding three BChl *a* molecules and one lycopene (a specific type of carotenoid). Presumably, there exists a second lycopene for each $\alpha\beta$ -heterodimer. The electron density map indeed contains a stretch of assignable density, but the stretch is not long enough to positively resolve the entire lycopene (19). Two concentric cylinders of α -helices, with the α -apoproteins inside and the β -apoproteins outside, form a scaffold for BChls and lycopenes. Fig. 3*b* depicts the 24 BChl molecules and 8 lycopene molecules in LH-II with all other components stripped away. Sixteen B850 BChl molecules form a continuous overlapping ring of 23 Å radius (based on central Mg atoms of BChls) with each BChl oriented perpendicular to the membrane plane. The Mg-Mg distance

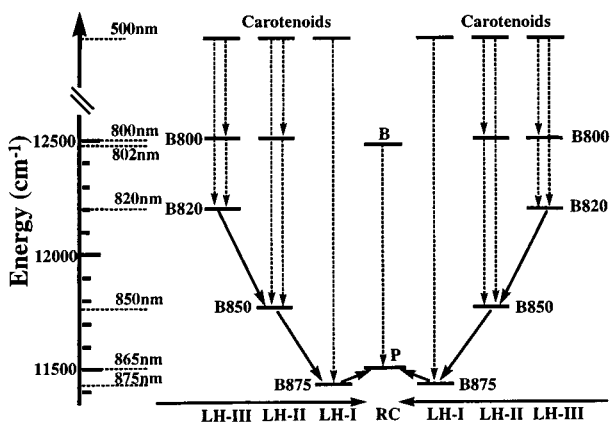


FIG. 2. Energy levels of the electronic excitations in the PSU of BChl *a* containing purple bacteria. The diagram illustrates a funneling of excitation energy toward the photosynthetic RC. The dashed lines indicate (vertical) intracomplex excitation transfer, and the solid lines (diagonal) indicate intercomplex excitation transfer. LH-I exists in all purple bacteria; LH-II exists in most species; LH-III arises in certain species only.

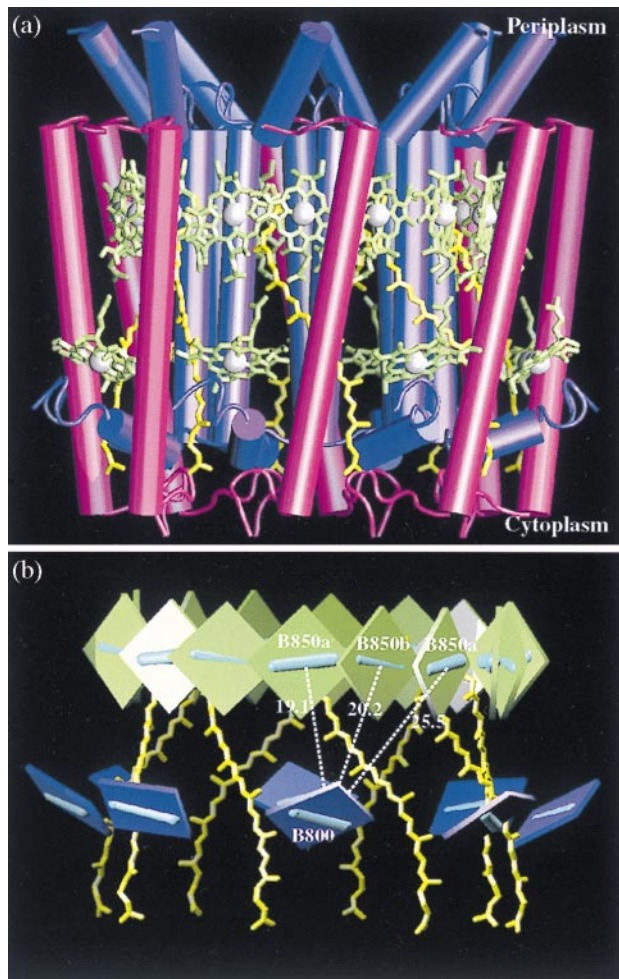


FIG. 3. The octameric LH-II complex from *Rs. molischianum* (19). (a) The α -helical segments are represented as cylinders with the α -apoproteins (inside) in blue and the β -apoprotein (outside) in magenta. The BChl molecules are in green with phytol tails truncated for clarity. The lycopenes are in yellow. (b) Arrangement of chromophores with BChls represented as squares, and with carotenoids (lycopenes) in a licorice representation. Bars connected with the BChls represent the Q_y transition dipole moments as defined by the vector connecting the N atom of pyrrol I and the N atom of pyrrol III (22). Representative distances between central Mg atoms of B800 BChl and B850 BChl are given in Å. The B850 BChls bound to the α -apoprotein and the β -apoprotein are denoted as B850a and B850b, respectively; BChl B850a' is bound to the (left) neighboring heterodimer.

between neighboring B850a and B850b BChls is 9.2 Å (within an $\alpha\beta$ -heterodimer) and between B850a' and B850b is 8.9 Å (between heterodimers). Eight B800 BChls, forming another ring of 28 Å radius, are arranged with their tetrapyrrol rings nearly parallel to the membrane plane and exhibit a Mg-Mg distance of 22 Å between neighboring BChls, i.e., the BChls are coupled only weakly. The ligation sites for the B850 BChls are α -His-34 and β -His-35, and the B800 BChls ligate to α -Asp-6. Eight lycopene molecules span the transmembrane region; each makes contact with B800 BChl and the B850a BChl.

It is remarkable that LH-II results from the self-aggregation of a large number of identical, noncovalently bonded transmembrane helices, BChls, and carotenoids. With its simple, symmetric architecture, LH-II constitutes an ideal model system for studying aggregate formation and adhesive interactions of proteins. Mechanical models reveal perfect self-complementarity of the $\alpha\beta$ -heterodimers that interlock with each other to form a circular aggregate (23).

LH-I-RC Complex. LH-I of *Rb. sphaeroides* has been modeled in ref. 21 as a hexadecamer of $\alpha\beta$ -heterodimers; the modeling exploited a close homology of these heterodimers to those of LH-II of *Rs. molischianum*. The resulting LH-I structure yields an electron density projection map that is in agreement with an 8.5 Å resolution electron microscopy projection map for the highly homologous LH-I of *Rs. rubrum* (24). The LH-I complex contains a ring of 32 BChls referred to as B875 BChls according to their main absorption band. The Mg–Mg distance between neighboring B875 BChls is 9.2 Å within the $\alpha\beta$ -heterodimer and 9.3 Å between neighboring heterodimers.

The modeled LH-I has been docked to the photosynthetic RC of *Rb. sphaeroides* by means of a constrained conformational search (21), employing for the latter the structure reported in ref. 17. Fig. 4*a* presents the LH-I-RC complex. The arrangement of the BChls in the LH-I-RC complex is depicted in Fig. 4*b*. One can discern the ring of B875 BChls of LH-I that surrounds the RC special pair (P_A and P_B) and the so-called accessory BChls (B_A , B_B). The closest distance between the central Mg atom of the RC's special pair (BChls P_A , P_B) and the Mg atom of the BChls in LH-I is 42.6 Å. The distance between the Mg atom of the accessory Bchl (BChls B_A , B_B) and the LH-I BChls is shorter, the nearest distance measuring

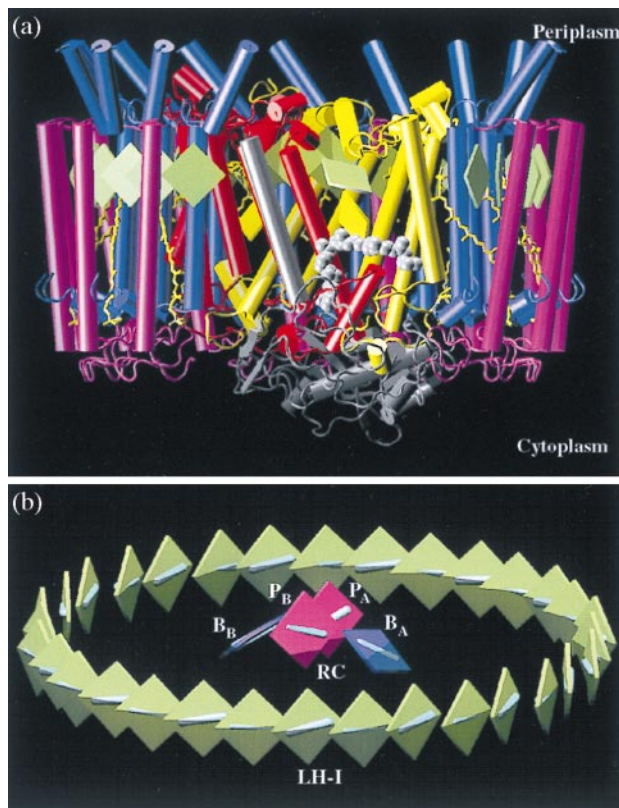


FIG. 4. Structure of the LH-I-RC complex. (a) Side view of the LH-I-RC complex with three LH-I $\alpha\beta$ -heterodimers on the front side removed to expose the RC in the interior. The α -helices are represented as cylinders with the L, M, and H subunits of the RC in yellow, red, and gray, and the α -apoprotein and the β -apoprotein of the LH-I in blue and magenta. BChls and bacteriopheophytins are represented as green and yellow squares, respectively. Carotenoids (spheroidenes) are in a yellow licorice representation, and quinone Q_B is rendered by gray van der Waals spheres. Q_B shuttles in and out (as Q_BH_2) of the LH-I-RC complex as indicated in Fig. 1. (b) Arrangement of BChls in the LH-I-RC complex. The BChls are represented as squares with B875 BChls of LH-I in green, and the special pair (P_A and P_B) and the accessory BChls (B_A and B_B) of the RC in red and blue, respectively; cyan bars represent Q_y transition moments of BChls. [Produced with the program VMD (25)].

35.7 Å. *Rb. sphaeroides* contains an additional *PufX* gene of unknown function. It has been suggested that the *PufX* protein may substitute one or more $\alpha\beta$ -heterodimers of LH-I to open up the circular ring shown in Fig. 4*a* and to facilitate thereby the flow of quinones (Q_B/Q_BH_2) between the RC and the cytochrome bc_1 complex (see Fig. 1) (4, 9).

The PSU. Fig. 5 presents a model of the PSU for *Rb. sphaeroides*. Only three LH-IIs are shown. The actual photosynthetic apparatus can contain up to about 10 LH-IIs around each LH-I. Because electron microscopy observations suggest that LH-II of *Rb. sphaeroides* contains nine $\alpha\beta$ -heterodimers (J. Olsen, personal communication), instead of eight as in LH-II of *Rs. molischianum*, LH-II of *Rb. sphaeroides*, as shown in Fig. 5, has been constructed as a nanomer of $\alpha\beta$ -heterodimers by means of homology modeling by using the $\alpha\beta$ -heterodimer of LH-II from *Rps. acidophila* as a template. For this purpose, the modeling protocol developed and applied successfully in refs. 19–21 was used.

Two essential features of the pigment organization of the PSU, as depicted in Fig. 5, are (i) the ring-like aggregates of tightly coupled BChls within LH-I and LH-II, and (ii) the coplanar arrangement of these BChls and of the BChls in the RC. Analysis of the LH-I and LH-II structures as reported in refs. 21 and 26 indicates that each Bchl of the B850 ring of LH-II and of the B875 ring of LH-I is noncovalently bound to three side-chain atoms of the α - or β -apoprotein such that the BChls are held in a rigid orientation. The planar organization of the BChls in the PSU is optimal for the transfer of electronic excitation to the RC.

Mechanisms of Excitation Transfer

Photosynthetic bacteria evolved a pronounced energetic hierarchy in the light-harvesting system. The hierarchy, as shown in Fig. 2, furnishes a cascade-like system of excited states that funnels electronic excitation from the outer LH-IIs through LH-I to the RC. The excitation transfer cascading into the RC involves intracomplex and intercomplex processes, defined as excitation transfer within each pigment–protein complex (LH-II, LH-I, RC) and between pigment–protein complexes (LH-II \rightarrow LH-II, LH-II \rightarrow LH-I, LH-I \rightarrow RC), respectively. Intracomplex transfer, for the main part, occurs faster than intercomplex transfer. We will first discuss intercomplex excitation transfer, and then we will describe intracomplex excitation transfer.

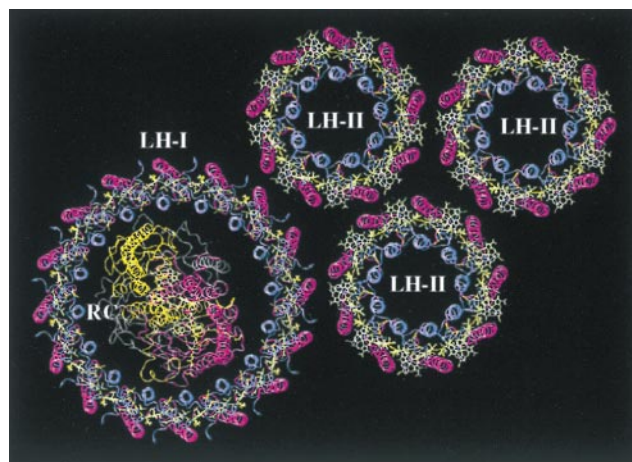


FIG. 5. Arrangement of pigment–protein complexes in the modeled bacterial PSU of *Rb. sphaeroides*. The α -helices are represented as C_α -tracing tubes with α -apoproteins of both LH-I and LH-II in blue and β -apoproteins in magenta, and the L, M, and H subunits of RC in yellow, red, and gray, respectively. All the BChls are in green, and carotenoids are in yellow. [Produced with the program VMD (25)].

Exciton Migration. One of the most intriguing structural features of the bacterial light-harvesting complexes is the circular organization of BChl aggregates (2). To understand the primary processes of light absorption and the subsequent excitation transfer from LH-II, through LH-I, to the RC, it is essential to characterize the electronic properties of the excited states of the circular BChl aggregate. The close proximity of the B850 BChls in LH-II implies strong interactions, leading to coherent superpositions, termed excitons (27, 28), of the lower energy excited states of individual BChls, the Q_y states as demonstrated in INDO-CIS level quantum chemical calculations of the complete circular aggregates of 16 B850 BChls and 8 B800 BChls of LH-II from *Rs. molischianum* (29). As shown in Fig. 6, two bands of excitons arise, with the band splitting reflecting a weakly dimerized form of the aggregate (the BChl-BChl distances alternate slightly along the ring) (26). Only 2 of the 16 exciton states are optically allowed and thus carry an 8-fold enhanced oscillator strength (superradiance); the lowest excited state is optically forbidden and does not fluoresce, which may allow LH-II to preserve excitation

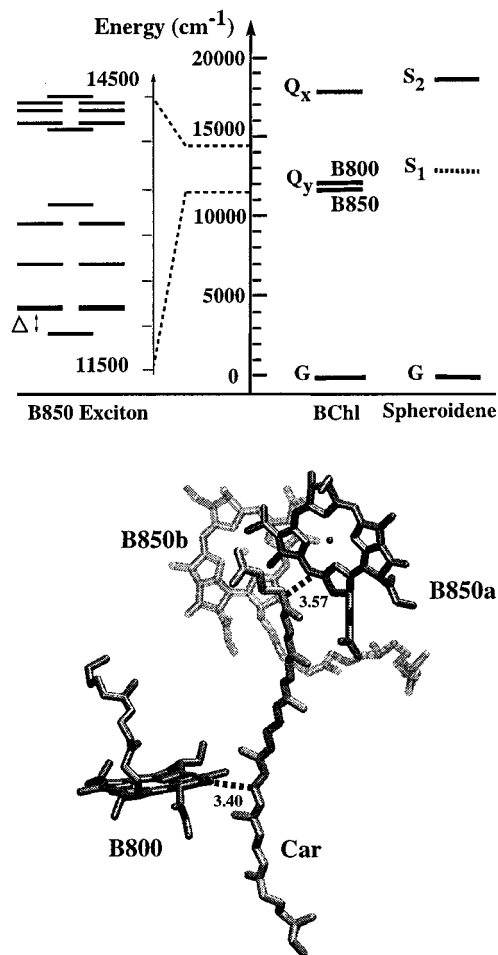


FIG. 6. BChl-carotenoid interactions. (Upper Left) Exciton bands of the circular B850 BChl aggregate as determined by quantum chemical (INDO/S) calculations (29) based on coordinates of the crystal structure of LH-II from *Rs. molischianum* (19). The degenerate states that carry all the oscillator strength are highlighted by thickened lines. (Upper Right) Excitation energies of BChl and carotenoid states in LH-II of *Rb. sphaeroides*. Solid lines represent spectroscopically measured energy levels. The dashed line indicates the estimated (see refs. 44 and 47) energy for the optically forbidden S_1 state of the carotenoid spheroidene. (Lower) Arrangement of spheroidene and the most proximate BChls based on the modeled structure of LH-II from *Rb. sphaeroides*. Close contacts between BChl and the carotenoid spheroidene are indicated by representative distances (in angstroms).

energy, though disorder confers readily oscillator strength to this state (26).

Other, less extensive calculations, ranging from an effective Hamiltonian representation based on the point dipole treatment (30, 31) to a point monopole treatment (32), and to the quantum mechanical consistent-force-field/ π -electron (QCF/PI) approach (33), yield a similar exciton band structure but differ in detailed exciton levels and band gaps. According to the INDO-CIS calculation (29), the lowest exciton state is significantly lowered in energy through level repulsion with charge resonance states, resulting in an energy gap Δ of 422 cm^{-1} (see Fig. 6). The optically allowed exciton states should then be populated 9% at thermal equilibrium at room temperature.

To extend the quantum chemical calculations to LH-I and the complete PSU, an effective Hamiltonian \hat{H} in the basis of single BChl Q_y excitations had been established in ref. 26. The matrix elements of the Hamiltonian describe couplings between neighboring Q_y states by $\langle j|\hat{H}|j+1\rangle$, assuming values of v_1 (v_2) for odd (even) j . The diagonal elements $\langle j|\hat{H}|j\rangle = \varepsilon$ account for the excitation energy of the Q_y state of individual BChls. All other elements of \hat{H} are approximated by dipole-dipole coupling terms

$$\langle j|\hat{H}|k\rangle = C \left(\frac{\vec{d}_j \cdot \vec{d}_k}{r_{jk}^3} - \frac{3(\vec{r}_{jk} \cdot \vec{d}_j)(\vec{r}_{jk} \cdot \vec{d}_k)}{r_{jk}^5} \right), k \neq j, j \pm 1,$$

where \vec{d}_j are unit vectors describing the direction of the transition dipole moments of the ground state $\rightarrow Q_y$ state transition of the j -th BChl and \vec{r}_{jk} is the vector connecting the centers of BChl j and BChl k . The adjustable parameters of the effective Hamiltonian were determined in ref. 29 to reproduce the exciton spectrum in Fig. 6: $\varepsilon = 13,242 \text{ cm}^{-1}$, $v_1 = 790 \text{ cm}^{-1}$, $v_2 = 369 \text{ cm}^{-1}$, and $C = 505,644 \text{ \AA}^3 \cdot \text{cm}^{-1}$. The effective Hamiltonian was extended in ref. 34 to incorporate two exciton states as they arise in pump-probe spectroscopy (35).

The effective Hamiltonian can be applied without further modification to describe the circular aggregate of 32 BChls in LH-I (26). The same characteristics of the exciton bands as in the B850 BChl aggregate of LH-II are found, i.e., the second and the third exciton states carry all the oscillator strength, with the lowest energy excitation state being optically forbidden.

The exciton states in LH-II and LH-I are completely delocalized over the ring-like B850 and B875 aggregates because of the assumption of perfect symmetry, i.e., absence of disorder. It is widely believed that the B850 BChl excited states, despite

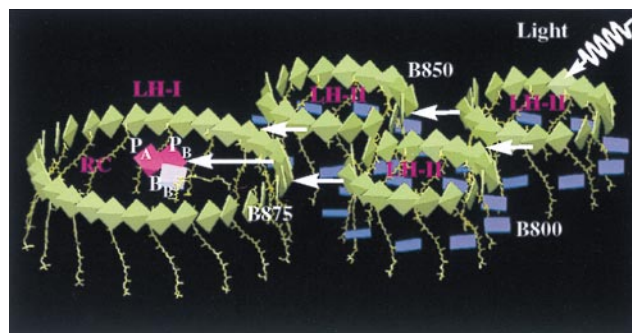


FIG. 7. Excitation transfer in the bacterial photosynthetic unit. LH-II contains two types of BChls, commonly referred to as B800 (dark blue) and B850 (green), which absorb at 800 nm and 850 nm, respectively. BChls in LH-I absorb at 875 nm and are labeled B875 (green). P_A and P_B refer to the RC special pair, and B_A , B_B refer to the accessory BChls in the RC. The figure demonstrates the coplanar arrangement of the B850 BChl ring in LH-II, the B875 BChl ring of LH-I, and the RC BChls P_A , P_B , B_A , B_B . [Produced with the program VMD (25)].

natural disorder, are delocalized, but the extent of delocalization has been debated (15). The estimate for the number of coherently coupled BChls ranges from two BChl molecules (36) to the entire length of the B850 BChl aggregate (37). In principle, the relative strengths of the disorder and of the coupling between BChls determine the delocalization length. According to the INDO-CIS calculation (29), the effective coupling between nearest neighbor BChls is 790 cm^{-1} (ν_1) within the $\alpha\beta$ -heterodimer and 369 cm^{-1} (ν_2) between the $\alpha\beta$ -heterodimers. The effect of static disorder has been modeled in ref. 26 by randomizing the diagonal elements of an effective Hamiltonian. By using a distribution consistent with the inhomogeneous broadening measured by hole-burning spectroscopy, the effect of diagonal disorder on exciton delocalization was found to be noticeable but small.

It has long been observed that excitation transfer LH-II \rightarrow LH-I \rightarrow RC occurs in the PSU in fewer than 100 ps and with about 95% efficiency (14). In this respect, it is interesting to note that the transition dipole moments of the Q_y excitations of the B850 and B875 BChls are all oriented in the two-dimensional plane that encompasses the ring-like BChl aggregates of LH-II, LH-I, and the RC special pair and is optimally attuned to the desired flow of electronic excitation LH-II \rightarrow LH-I \rightarrow RC. There are many potential pathways for photons to be absorbed and for the subsequent excitations to reach the RC. A path may begin with absorption of an 800 nm photon by one of the B800 BChls in LH-II (see Fig. 7). At least three sequential steps are required for the B800 excitation to be transferred to the RC: B800 (LH-II) \rightarrow B850 (LH-II) \rightarrow LH-I \rightarrow RC. Time resolved picosecond and femtosecond spectroscopy revealed that the B800 \rightarrow B850 excitation transfer proceeds within about 700 fs (14, 38). Two color pump-probe femtosecond measurements determined a time constant of 3–5 ps for the B850 \rightarrow LH-I step (39). The final LH-I \rightarrow RC transfer step requires about 35 ps (40), i.e., this is the slowest step (11, 14). Intercomplex LH-II \rightarrow LH-II transfer may occur, but a rate for this process has not yet been determined.

The effective Hamiltonian for LH-II, as described above, had been extended in refs. 26 and 34 to describe the exciton system of the entire aggregate shown in Fig. 7. One can determine the transfer rates between the different components, i.e., LH-II \rightarrow LH-I, and LH-I \rightarrow RC, by using a perturbation scheme (34). The calculated time constants of 3.3 and 65 ps for the excitation transfer processes LH-II \rightarrow LH-I and LH-I \rightarrow RC in *Rb. sphaeroides*, respectively, are in agreement with experimental values of 3–5 ps and 35 ps (39, 40). A startling result from these calculations has been a suggested role of the accessory BChls as mediators of the excitation transfer from LH-I to the RC special pair: the calculated time for LH-I \rightarrow RC transfer, in the absence of accessory BChls, is about 600 ps, which is an order of magnitude too long compared with observations; the accessory BChls in RC provide a path for the excitation transfer that bridges the large distance of 42 Å or longer between LH-I BChls and the RC special pair.

Role of B800 BChls and Carotenoids. B800 BChls absorb light in a slightly higher spectral region than the B850 BChls and are oriented such that they absorb in a direction perpendicular to that of the B850 BChls. Quantum chemical calculations in ref. 29 have demonstrated that the B800 BChls are only weakly coupled with each other and with the B850 BChls. The individual B800 BChls transfer the resulting excitation energy to the B850 ring through the so-called Förster mechanism (41–43). The transfer proceeds within 700 fs (38). Quantum mechanical calculations show that this short transfer time, to a large degree, results through the exciton splitting of the accepting B850 exciton levels shown in Fig. 6; the exciton splitting greatly improves the resonance of the excitations of B800 and B850 BChls (44). Carotenoids absorb light at 500 nm into a strongly allowed state and transfer the excitation energy

within 200 fs and with nearly 100% efficiency to the Q_y exciton states of the B850 ring (45). The question arises by which pathways and by which mechanism such an efficient excitation transfer is achieved.

Fig. 6 presents also the excitation energies of the spheroidene and BChl states in LH-II of *Rb. sphaeroides*. Spheroidene features two low-lying singlet excited states. A strongly allowed state absorbing at 500 nm is labeled S_2 . It decays within <200 fs into an optically forbidden electronic state labeled S_1 , which has been characterized in refs. 46 and 47. The S_1 state is in resonance with the accepting Q_y exciton states and, thus, provides a possible gateway for transfer to the B850 ring.

The optically forbidden character of the S_1 state of spheroidene precludes its coupling to the B850 ring through the Förster mechanism, thus limiting potential mechanisms to coupling through Coulomb interaction including higher-order multipoles (generalized Förster mechanism) or coupling through electron exchange [Dexter mechanism (48)]. The Dexter mechanism requires an overlap of donor and acceptor wave functions and, thus, is only efficient when donor and acceptor are in van der Waals contact. Because spheroidene and BChls are indeed in close contact, as shown in Fig. 6, one is tempted to suggest that the mechanism underlying singlet excitation transfer is electron exchange.

Recent calculations (44, 49), however, do not support this assumption. Based on the geometric arrangement of carotenoids and BChls in LH-II (Fig. 6) and on CI expansions of the electronic states of carotenoids and chlorophylls, calculations in ref. 44 showed that the generalized Förster mechanism governs the transfer of singlet excitations, resulting in a transfer time of 260 fs through the S_1 (carotenoid) \rightarrow B850 (exciton states) pathway.

The transfer through the optically forbidden S_1 state is strongly accelerated by the splitting of the B850 exciton levels as seen also in the case of the B800 \rightarrow B850 transfer (44). Without the exciton splitting, the calculated transfer time is as slow as 2.5 ps. This suggests that purple bacteria may have evolved the ring structure of LH-II to improve resonance between acceptor and donor systems. In addition to transfer through the forbidden S_1 state of spheroidene, the absorbing S_2 state of carotenoids is likely to transfer some excitation also directly to the Q_x state of BChl as suggested by the calculated transfer time of 330 fs (44) and the shortened (60 fs) *in vivo* lifetime of the S_2 state (50).

In addition to the light-harvesting function, carotenoids protect the light-harvesting system from the damaging effect of BChl triplet states that arise with a small, but finite, probability and can generate highly reactive singlet oxygen according to the reaction ${}^3\text{O}_2 + {}^3\text{BChl}^* \rightarrow {}^1\text{O}_2 + {}^1\text{BChl}$. Carotenoids prevent this reaction by quenching the BChl triplet states through triplet excitation transfer from the BChls. This transfer involves a spin change and can only proceed through the electron exchange or Dexter mechanism (48). The triplet excitation transfer in LH-II of *Rs. molischianum* has been described in detail (44). The calculations showed that B850a and B800 are well protected by one of the eight lycopenes seen in the crystal structure of LH-II of *Rs. molischianum* (see Figs. 3 and 6), whereas B850b is not directly protected but can transfer triplet excitation within a few picoseconds to the well protected B850a BChl.

Other Photosynthetic Organisms

Photosynthetic organisms have developed from a few common components a rather divergent set of antenna systems. The divergence is demonstrated in Fig. 8, which compares antenna systems of green bacteria, cyanobacteria, dinoflagellates, and green plants; to these examples is to be added the apparatus of purple bacteria shown in Fig. 1.

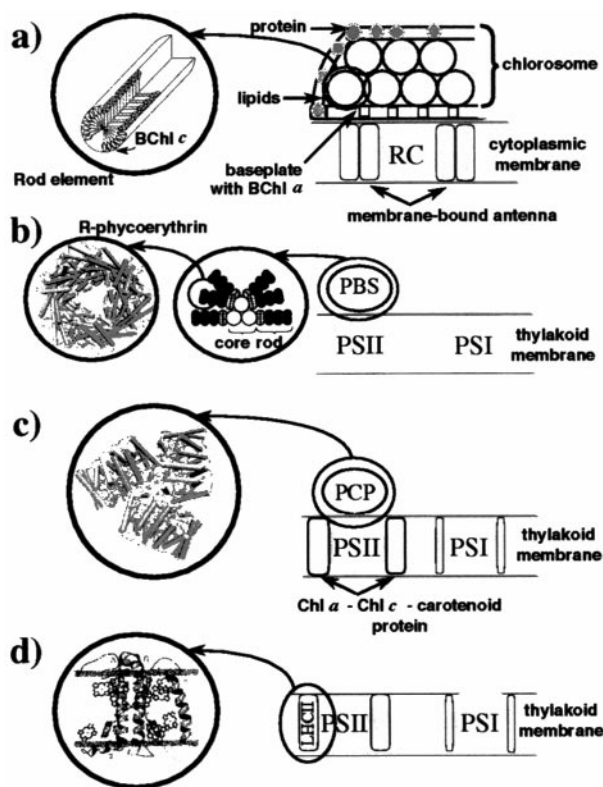


FIG. 8. Schematic representation of proposed models of the PSUs in other photosynthetic systems. The figure displays inter- and extramembrane light-harvesting complexes, together with the RCs (RC in green bacteria, and PS-I and PS-II in cyanobacteria, dinoflagellates, and green plants). (a) Green bacteria: The major light-harvesting complex, chlorosome, contains rod-like BChl *c* aggregates surrounded by a layer of protein embedding lipids. Excitation energy harvested by the rod-like aggregates reaches the RC through a BChl *a* containing baseplate and membrane-bound light-harvesting BChl *a* complexes. (b) Cyanobacteria: The dominant light-harvesting complex of cyanobacteria and red algae, phycobilisome (PBS), is unique in choosing linear tetrapyrroles as pigments. Several types of disk-like pigment-protein complexes such as R-phycoerythrin (51) constitute the phycobilisome rods and core. (c) Dinoflagellates: The photosynthetic unit of dinoflagellates consists of several membrane-bound pigment-protein complexes and an extramembrane light-harvesting complex, the peridinin-chlorophyll-protein (PCP). (d) Green plants: Chloroplasts of green plants possess chlorophyll-carotenoid containing LH-CII (6) as the most abundant light-harvesting complex. [Images of R-phycoerythrin and PCP were produced with the program VMD (25)].

Anoxygenic photosynthetic (purple and green) bacteria employ a single RC. Oxygen-evolving photosynthetic organisms, e.g., cyanobacteria, dinoflagellates, and plants, possess in their PSUs two RCs of different types, namely PS-I and PS-II (see Figs. 8 *b*, *c*, and *e*). PS-I shows similarity to the RCs of green sulfur bacteria, whereas PS-II is thought to be evolutionary related to the RC of purple bacteria. PS-I and PS-II have integral light-harvesting pigments associated with them (5). Apart from those integral light-harvesting pigments, oxygen-evolving photosynthetic organisms possess additional light-harvesting complexes that display significant structural variability among species.

To illustrate the common components of the light-harvesting systems in Figs. 1 and 8, we summarize the properties of the antenna systems of purple bacteria as far as they are relevant to photosynthetic life forms in general.

The chromophores of purple bacteria, i.e., BChls and carotenoids, are attuned to their ambient light. In case of lycopene/spheroidene and B800/B850 BChls, the combined absorption spectrum is complementary to that of chlorophyll *a* or *b* in

green plants, i.e., adjusted to a habitat below plants. The purple bacteria exploit the low-lying excited states of polyenes (46, 47) to couple the carotenoid excitations to BChls. The carotenoids are entrusted with the excitation energy for only a few hundred femtoseconds, after which time BChls are the wardens of the energy.

The spectra of BChls are tuned only to a limited degree through interaction with the protein environment, e.g., through formylmethionine-Mg ligation in case of B800 of LH-II from *Rps. acidophila* (18) or through an Asp-Mg ligation in case of B800 of LH-II from *Rs. molischianum* (19); the observed spectra result mainly from intrinsic properties of BChls and excitonic interactions (26, 29). Excitonic coupling splits the excited state energies, thus improving the overlap between donor and acceptor spectra in the excitation cascade (26, 41, 44).

The BChls have the disadvantage that their lowest-energy triplet state lies high enough to excite molecular oxygen. Their companion carotenoids quench the triplet excitations of BChls.

The efficient flow of excitation through the chromophore system requires highly ordered aggregates, the geometry of which is adapted to the needed interactions; carotenoids must be in close (van der Waals) contact with BChls for triplet quenching and must be proximate within a few angstroms for transfer of optically forbidden excitations. Chlorophylls, to achieve significant exciton splitting, must have Mg-Mg distances of about 10 Å; for energy transfer on a picosecond time scale, Mg-Mg distances must be of the order of 20 Å. It is possible that BChls form aggregates to achieve coherence over many chromophores, such that the lowest-energy state becomes optically forbidden, increasing its lifetime.

A multiprotein architecture is necessary to provide a large enough scaffold for the number of chromophores employed in light harvesting. Because of this architecture, antenna systems employ a hierarchy of chromophore aggregates; the chromophores are closer and more tightly coupled in the individual pigment-protein complex, e.g., in LH-II, and more loosely coupled between different pigment-protein complexes. The control of the overall aggregation of the multiprotein system is in itself an impressive achievement worthy of study (23).

To direct flow of excitation to the RC, the antenna system of purple bacteria assumes a spatial organization in which the BChls with lower energy excitations are closer to the RC. Such arrangement, as shown in Fig. 2, yields an energy funnel that prevents detours in the excitation flow, enhancing the overall efficiency of light harvesting as measured by the quantum yield for a photon absorbed to reach a RC.

The features of light harvesting in purple bacteria can serve as a background to a comparison of the alternative antenna systems shown in Fig. 8. As their primary light-harvesting complexes, green bacteria use extramembrane sack-like aggregates of BChl *c* (*d* or *e* in some species) called chlorosomes (Fig. 8*a*). Chlorosomes consist of pigment oligomers which in some species appear to be rod-shaped aggregates of BChls. It has been suggested that the rod-shaped BChl aggregates are stabilized solely through pigment-pigment interactions between the BChls. Chlorosomes are positioned external to the membrane, on top of the RC as shown in Fig. 8*a*.

In cyanobacteria and red algae, the dominant light-harvesting complexes, shown in Fig. 8*b*, are extramembrane PBSs with discoidal pigment-protein complexes exhibiting an energy cascade from the outer rod disks toward the core and the RC.

The PSU of dinoflagellates, presented in Fig. 8*c*, contains, among other pigment-protein complexes, the extramembrane PCP. Recently, the structure of PCP has been solved at 2.0 Å resolution (52). PCP distinguishes itself from other light-harvesting complexes in using carotenoids as the predominant light absorbers, exhibiting a chlorophyll-to-carotenoid ratio of

1:4. Efficient excitation transfer between carotenoids and chlorophylls, based on the structure of the aggregate, i.e., close contacts between peridinin and chlorophylls, has been confirmed by quantum chemical calculations (T.R., A.D., and K.S., unpublished work).

The most abundant light-harvesting complex located in chloroplasts of green plants is LHCII, shown in Fig. 8*d*. The structure of LHCII, resolved at 3.4 Å (6), features two carotenoids, seven Chls *a*, and five Chls *b* as light-absorbing agents. LHCII is located within the thylakoid membrane in the vicinity of PS-II. It has been suggested that LHCII can, according to light conditions, physically move toward PS-I, regulating thereby the relative flow of energy into PS-II and PS-I.

The multiprotein photosynthetic apparatus as shown in Fig. 1 poses the challenge for eventually modeling the conversion of light into ATP in its entirety. Few would have predicted that the protein constituents of the photosynthetic apparatus would be structurally known in principle already today, but many expect that biologists will see more and more often entire protein systems engaged in complex overall functions resolved at atomic resolution. The questions posed by the photosynthetic apparatus will then be typical for biology of the 21st century: how are multiprotein systems genetically controlled, how do they physically aggregate, how did they evolve, and how do they compare between species? The PSU constitutes an ideal subsystem of the photosynthetic apparatus that, because of its smaller size, is more amenable to study while posing the same principal challenges: how do LH-I and LH-II form from their many independent components, what determines the ring size and stability, and how do the completed LH-IIs aggregate around the LH-I-RC complex? The function of the PSU emerges as a true system property, all components being designed to cooperate in absorbing light effectively and channel its energy to the RC. The common origin of photosynthetic, respiratory, and other organisms makes the PSU and the photosynthetic apparatus a valuable model for understanding, at the level of multiprotein systems, not only photosynthesis but also life in general.

We acknowledge financial support from the National Institutes of Health [Grant P41RR05969], the National Science Foundation [Grants NSF BIR 9318159 and NSF BIR-94-23827(EQ)], and the Carver Charitable Trust.

- Emerson, R. & Arnold, W. (1932) *J. Gen. Physiol.* **16**, 191–205.
- Hu, X. & Schulten, K. (1997) *Physics Today* **50**, 28–34.
- Duysens, L. N. M. (1952) Ph.D. thesis (Utrecht, The Netherlands).
- Cogdell, R., Fyfe, P., Barrett, S., Prince, S., Freer, A., Isaacs, N., McGlynn, P. & Hunter, C. (1996) *Photosynth. Res.* **48**, 55–63.
- Krauss, N., Schubert, W.-D., Klukas, O., Fromme, P., Witt, H. T. & Saenger, W. (1996) *Nat. Struct. Biol.* **3**, 965–973.
- Kühlbrandt, W., Wang, D.-N. & Fujiyoshi, Y. (1994) *Nature (London)* **367**, 614–621.
- Zuber, H. & Brunisholz, R. A. (1991) in *Chlorophylls*, ed. Scheer, H. (CRC, Boca Raton, FL), pp. 627–692.
- Miller, K. (1982) *Nature (London)* **300**, 53–55.
- Walz, T. & Ghosh, R. (1997) *J. Mol. Biol.* **265**, 107–111.
- Monger, T. & Parson, W. (1977) *Biochim. Biophys. Acta* **460**, 393–407.
- van Grondelle, R., Dekker, J., Gillbro, T. & Sundstrom, V. (1994) *Biochim. Biophys. Acta* **1187**, 1–65.
- Germeroth, L., Lottspeich, F., Robert, B. & Michel, H. (1993) *Biochemistry* **32**, 5615–5621.
- Aagaard, J. & Siström, W. (1972) *Photochem. Photobiol.* **15**, 209–225.
- Pullerits, T. & Sundstrom, V. (1996) *Acc. Chem. Res.* **29**, 381–389.
- Fleming, G. R. & van Grondelle, R. (1997) *Curr. Opin. Struct. Biol.* **7**, 738–48.
- Deisenhofer, J., Epp, O., Miki, K., Huber, R. & Michel, H. (1985) *Nature (London)* **318**, 618–624.
- Ermiler, U., Fritzsche, G., Buchanan, S. K. & Michel, H. (1994) *Structure* **2**, 925–936.
- McDermott, G., Prince, S., Freer, A., Hawthornthwaite-Lawless, A., Papiz, M., Cogdell, R. & Isaacs, N. (1995) *Nature (London)* **374**, 517–521.
- Koepke, J., Hu, X., Münke, C., Schulten, K. & Michel, H. (1996) *Structure* **4**, 581–597.
- Hu, X., Xu, D., Hamer, K., Schulten, K., Koepke, J. & Michel, H. (1995) *Protein Sci.* **4**, 1670–1682.
- Hu, X. & Schulten, K. (1998) *Biophys. J.*, in press.
- Gouterman, M. (1961) *J. Mol. Spectrosc.* **6**, 138–163.
- Bailey, M., Schulten, K. & Johnson, J. E. (1998) *Curr. Opin. Struct. Biol.*, in press.
- Karrasch, S., Bullough, P. A. & Ghosh, R. (1995) *EMBO J.* **14**, 631–638.
- Humphrey, W. F., Dalke, A. & Schulten, K. (1996) *J. Mol. Graphics* **14**, 33–38.
- Hu, X., Ritz, T., Damjanović, A. & Schulten, K. (1997) *J. Phys. Chem. B* **101**, 3854–3871.
- Frenkel, J. (1931) *Phys. Rev.* **37**, 17–44.
- Knox, K. (1963) *Theory of Excitons* (Academic, New York).
- Zerner, M. C., Cory, M. G., Hu, X. & Schulten, K. (1998) *J. Phys. Chem. B.*, in press.
- Dracheva, T. V., Novoderezhkin, V. I. & Razjivin, A. (1996) *FEBS Lett.* **387**, 81–84.
- Hu, X., Xu, D., Hamer, K., Schulten, K., Koepke, J. & Michel, H. (1995) in *Biological Membranes: A Molecular Perspective from Computation and Experiment*, eds. Merz, K. & Roux, B. (Birkhäuser, Cambridge, MA), pp. 503–533.
- Sauer, K., Cogdell, R. J., Prince, S. M., Freer, A., Isaacs, N. W. & Scheer, H. (1996) *Photochem. Photobiol.* **64**, 564–576.
- Alden, R., Johnson, E., Nagarajan, V., Parson, W., Law, C. & Cogdell, R. (1997) *J. Phys. Chem. B* **101**, 4667–4680.
- Ritz, T., Hu, X., Damjanović, A. & Schulten, K. (1998) *J. Lumin.*, **76–77**, 310–321.
- Pullerits, T., Sundstrom, V. (1996) *J. Phys. Chem.* **100**, 10787–10792.
- Jimenez, R., Dikshit, S., Bradforth, S. & Fleming, G. (1996) *J. Phys. Chem.* **100**, 6825–6834.
- Wu, H.-M., Reddy, N. R. S. & Small, G. J. (1997) *J. Phys. Chem. B* **101**, 651–656.
- Shreve, A. P., Trautman, J. K., Frank, H. A., Owens, T. G. & Albrecht, A. C. (1991) *Biochim. Biophys. Acta* **1058**, 280–288.
- Hess, S., Chachisvilis, M., Timpmann, K., Jones, M. R., Fowler, G. J. S., Hunter, C. N. & Sundstrom, V. (1995) *Proc. Natl. Acad. Sci. USA* **92**, 12333–12337.
- Visscher, K. J., Bergstrom, H., Sundstrom, V., Hunter, C. N. & van Grondelle, R. (1989) *Photosynth. Res.* **22**, 211–217.
- Arnold, W. & Oppenheimer, J. R. (1950) *J. Gen. Physiol.* **33**, 423–435.
- Oppenheimer, J. R. (1941) *Phys. Rev.* **60**, 158.
- Förster, T. (1948) *Ann. Phys. (Leipzig)* **2**, 55–75.
- Damjanović, A., Ritz, T. & Schulten, K. (1998) *Phys. Rev. E.*, in press.
- Chadwick, B. W., Zhang, C., Cogdell, R. J. & Frank, H. A. (1987) *Biochim. Biophys. Acta* **893**, 444–457.
- Hudson, B. S., Kohler, B. E. & Schulten, K. (1982) in *Excited States*, ed. Lim, E. C. (Academic, New York), Vol. 6, pp.1–95.
- Tavan, P. & Schulten, K. (1987) *Phys. Rev. B* **36**, 4337–4358.
- Dexter, D. L. (1953) *J. Chem. Phys.* **21**, 836–850.
- Nagae, H., Kakitani, T., Katoh, T. & Mimuro, M. (1993) *J. Chem. Phys.* **98**, 8012–8023.
- Ricci, M., Bradforth, S. E., Jimenez, R. & Fleming, G. R. (1996) *Chem. Phys. Lett.* **259**, 381–390.
- Chang, W., Jiang, T., Wan, Z., Zhang, J., Yang, Z. & Liang, D. (1996) *J. Mol. Biol.* **262**, 721–731.
- Hofmann, E., Wrench, P., Sharples, F., Hiller, R., Welte, W. & Diederichs, K. (1996) *Science* **272**, 1788–1791.